



Silver nanoparticles impregnated with polyamide-66 to disinfect drinking water

ARTICLES doi:10.4136/ambi-agua.1947

Received: 19 Jun. 2016; Accepted: 12 Oct. 2018

**Luciano André Deitos Koslowski^{1*}; André Lourenço Nogueira²;
Silvana Licodiedoff¹; Adrieny Taliny Comper³; Marilena Valadares Folgueras⁴**

¹Universidade do Estado de Santa Catarina (UDESC), Ibirama, SC, Brasil
Centro de Educação Superior do Alto Vale do Itajaí (CEAVI). Departamento de Engenharia Sanitária.
E-mail: lucianoandre@yahoo.com, siolico@yahoo.com.br

²Universidade da Região de Joinville (UNIVILLE), Joinville, SC, Brasil
Programa de Pós-Graduação em Engenharia Processos. E-mail: andre.nogueira@univille.br

³Universidade do Estado de Santa Catarina (UDESC), Ibirama, SC, Brasil
Centro de Educação Superior do Alto Vale do Itajaí (CEAVI). E-mail: adri.comper@hotmail.com

⁴Universidade do Estado de Santa Catarina (UDESC), Joinville, SC, Brasil
Programa de Pós-Graduação em Engenharia de Materiais. Departamento de Engenharia Mecânica.
E-mail: marilena.folgueras@udesc.br

*Corresponding author

ABSTRACT

The importance of the preservation of water resources has resulted in the application of technologies such as nanostructured materials, which are able to minimize the impact associated with water contamination. This work evaluated the application of polyamide-66 (PA) pellets functionalized with silver nanoparticles (AgNPs) at polymer mass percentages of 0.05, 0.10 and 0.50% to disinfect of drinking water. Studies were carried out in three stages. The first stage was the synthesis of the silver nanoparticles by using silver nitrate as a metal precursor and sodium borohydrate as a reduction agent. The colloidal dispersion was characterized by UV-Vis spectrophotometry and transmission electron microscopy (MET). Afterwards, the nanostructures were incorporated into a polyamide-66 polymeric matrix. In the second stage, the silver ions leached from the polymer matrix in the water after a three-hour period were quantified in order to evaluate the limit established by Conama Resolution 357/2005, which imposes a concentration limit of 0.010 mg L⁻¹. The best results were obtained with the application of 0.05% AgNPs in the polymeric matrix, yielding an average concentration of silver ions lixiviated of 0.008 mg L⁻¹. The last step comprised the quantification of the antibacterial activity of the polymer matrix containing 0.05% of AgNPs against the microorganism *E. coli* using the Standard Test Method for Determining the Antimicrobial Agents Under Dynamic Contact Conditions. The samples containing 0.05% of AgNPs exhibited an antibacterial reduction of 97.89% after 24 h of incubation under stirring at room temperature (25°C).

Keywords: *E. coli.*, polyamide-66, silver nanoparticles, water disinfection.



Uso de nanopartículas de prata impregnadas em poliamida-66 para desinfecção de água para consumo

RESUMO

A importância da preservação dos recursos hídricos tem resultado na aplicação de tecnologias, tais como o uso de materiais nanoestruturados, para minimizar o impacto associado à contaminação da água. Neste trabalho, foi avaliada a aplicação de *pellets* de poliamida-66 (PA) funcionalizados com nanopartículas de prata (AgNPs), em percentuais de 0.05; 0.10 e 0.50% em relação à massa de polímero, na desinfecção de água para consumo. O presente estudo teve como principal objetivo sintetizar as nanopartículas de prata, e avaliar a atividade antibacteriana destas nanoestruturas em relação à bactéria Gram negativa *Escherichia coli* quando incorporadas numa matriz de PA. A síntese das nanopartículas de prata foi realizada empregando o nitrato de prata como sal do metal precursor e o borohidreto de sódio como agente redutor. A dispersão coloidal foi caracterizada por espectrofotometria na região UV-Vis e microscopia eletrônica de transmissão. Posteriormente, foi realizada a quantificação de íons prata lixiviada da matriz polimérica para a água no período de 3 horas, de forma a avaliar comparativamente ao limite estabelecido pela Resolução do Conama 357/2005, que impõe um limite de concentração da prata de 0.010 mg L⁻¹. O melhor resultado consistiu na aplicação de 0.05% de AgNPs na matriz polimérica, lixiviando uma quantidade equivalente a uma concentração média de íons prata de 0.008 mg L⁻¹. A última etapa foi a utilização da matriz polimérica funcionalizada com as AgNPs em ensaios microbiológicos para mensurar a atividade antibacteriana do produto obtido contra o microrganismo *E. coli*. Os resultados ilustram que após 24 h de incubação, sob agitação e temperatura de 25°C, as amostras com 0.05% de AgNPs apresentaram uma redução antibacteriana de 97,89%.

Palavras-chave: desinfecção da água, *E. coli.*, nanopartículas de prata, poliamida-66.

1. INTRODUCTION

Drinking water sources are becoming increasingly scarce as a result of prolonged droughts and water pollution (Vörösmarty et al., 2000). Nascimento and Araújo (2013) reported that freshwater quality has been compromised due to anthropogenic actions mainly related to the disposal of sewage, which may contain a range of microorganisms natural to the human intestinal microbiota, such as members of the Enterobacteriaceae family. Pollution and water contamination increase the need for measures to mitigate environmental impact so that the application and optimisation of technologies for the adequate treatment of water are not compromised (Araújo et al., 2016).

Nanotechnology has attracted significant interest from several research areas in relation to the application of nanomaterials. In the medical field, metallic nanoparticles and their oxides have been proven effective against microorganisms (Nogueira et al., 2014; Kim et al., 2016).

In recent years, several studies have been undertaken on the application of silver nanoparticles in water disinfection, aiming at improving conventional water treatments (Zhang and Oyanedel-Craver, 2013). Such studies have reported the antimicrobial activity of silver nanoparticles against bacteria such as *Escherichia coli*, *Pseudomonas aeruginosa* and *Salmonella typhi* (Alizadeh et al., 2014). The action mechanisms and toxicity have been attributed to the interaction of Ag⁺ ions with sulphuric groups in the cell membrane of the microorganisms (Durán et al., 2016). Silver ions are of limited antimicrobial application due to their high toxicity and low stability. However, these drawbacks can be overcome by replacing Ag⁺ ions with properly stabilized silver nanoparticles (Mohanty et al., 2012).

Recent research indicates that silver nanoparticles act on the surface of the cell membrane and diffuse into the bacterium (Durán et al., 2016). There are some non-conclusive hypotheses about the mechanism of action of this nanostructure, including that silver might exhibit a synergistic action rather than a restrictive mode of action in relation to its antibacterial activity (Mohanty et al., 2012). Therefore, the objective of this study was to present a viable alternative for water disinfection using silver nanoparticles (AgNPs) incorporated in a polyamide-66 (PA) matrix as a bactericidal material.

2. MATERIAL AND METHODS

2.1. Silver nanoparticles (AgNPs) synthesis

In the literature, the synthesis of silver nanoparticles comprise different production methods, varying types and quantities of reactants, reaction time, stirring rate, heating, among other parameters. The preparation of these nanostructures relies on the use of aqueous solutions of silver salts – reducing and stabilizer agents – which are heated under stirring for a certain time (Polte et al., 2012). Variables such as the type and concentration of reactants (precursor salt and reducing agent) and stabilizers, pH and temperature have significant impact on particle size and morphology (Nogueira et al., 2014).

In this work, synthesis reactions of silver nanoparticles were conducted in a boron-silicate reactor with a 200-mL capacity, operating in a semi-continuous regime under controlled temperature and stirring. The silver nanoparticles were synthesized by initially adding 180 mL of deionized water to the reactor. Then, the precursor metal salt (silver nitrate – AgNO₃, Cennabras, Brazil) was added to the water until a concentration in the reaction medium equal to 9.3 mmol L⁻¹ was reached. The stabilizing agent employed to stabilize the colloidal dispersion (silver nanoparticles) was a hydrosoluble silicone wax containing amine functional groups (Quimisa, Brazil).

The concentration of this compound in the reaction medium was 0.84 g L⁻¹. The operational temperature was set at 20 °C and a stirring rate of 600 rpm was kept for 10 min to ensure complete solubilization. Then, 20 mL of a sodium borohydride solution (Nuclear, Brazil), with a concentration of 4.64 g L⁻¹ and a temperature of 10°C was added at an approximate flow rate of 1.5 mL min⁻¹. Following the addition of the reducing agent, the system was kept under temperature and stirring control for additional 10 min to ensure completion of the reaction.

In the next step, silica powder (Syloid 244 FD, 5 µm average diameter, Grace Division) was added to the metallic silver colloidal dispersion at the ratio of 1.0 g of silica to 8.0 mL of colloidal dispersion. The resulting suspension was kept under stirring for 30 minutes. Afterwards, the system was left to rest to allow the sedimentation of the silica particles to functionalize the silver nanoparticles. The silica was separated from the supernatant using a separator funnel and the solid material was dried at 50°C for 48 h.

The incorporation of the AgNP-containing powder into polyamide-66 was performed in the extruder illustrated in Figure 1a (Cristal Master Model GR 001) operating at 250°C at a dosing speed of 12.60 min⁻¹. The polyamide (PA) filaments incorporated with AgNPs were processed in a granulator (SAGEC Model S650/2) (Figure 1b) for the production of functionalized pellets with approximate area of 1.0 cm² and mass 0.25 g. PA/AgNPs pellets were produced at concentrations of 0.05%, 0.10% and 0.50% in relation to the weight of the silica powder incorporated with AgNPs.



Figure 1. (a) Extruder used to obtain PA/AgNPs filaments; (b) Granulator used to obtain PA/AgNPs pellets.

2.2. Characterization of nanoparticles

MET analyses were performed to evaluate the mean size, size distribution and geometric shape of the synthesized nanoparticles. Ten drops of silver nanoparticles dispersed in water were dripped onto a 300-mesh grid covered with carbon film. After drying at room temperature, the grids were examined in a microscope (JEOL, JEM-2100) and the images were captured at a voltage of 200 kV.

UV-Vis spectrophotometry analyses were conducted to obtain information on the optical properties of the synthesized product by absorption spectra. Thus, 0.1 mL of the AgNPs colloidal dispersion were diluted in 7.5 mL of deionized water, and 3.0 mL of this solution were added into a glass cuvette with a 10 mm optical path to obtain the absorption spectra in a spectrophotometer (Schimadzu, model UVPC-V.3.9). The UV-Vis tests were performed in triplicate and the same solution was prepared three times to ensure reproducibility of the results.

2.3. ICP-MS essays

The ICP-MS technique (Optima 8300 Perkin-Elmer) was selected to quantify the concentration of silver ions leached from the PA/AgNPs pellets after 3 h of contact with water samples contaminated with *E. coli*. The silver quantification was undertaken with solutions used in microbiological tests in the presence of silver nanoparticles, according to the methodology recommended in the Standard Methods for the Examination of Water and Wastewater (22nd ed.), methods SMEWW-3120 B and SMEWW-3030 E. Samples containing 0.05%, 0.10% and 0.50% of silica powder incorporated with AgNPs were prepared for the determination of Ag^+ ions by addition of rhodium as internal standard at concentration $5 \mu\text{g L}^{-1}$ and 1% (v/v) HNO_3 . The same methodology was used for the calibration and control solutions. The pneumatic nebulization was performed with argon gas (99.99% purity) to avoid interference in the tests.

2.4. Microbiological tests

For the analysis of faecal coliforms, Gram-negative bacteria *E. coli* (CCT-8739) was selected as faecal origin bacteria because it is directly related to health problems associated with contaminated water consumption. Faecal coliform analysis of water potability was performed using the Multi-Tube Fermentation Technique (TFTM) as described by APHA (2012). Serial dilutions were prepared and the medium to be analysed was transferred to test tubes containing the appropriate culture medium and a gas-collecting tube (Durhan tube). Following incubation

of the tubes, the samples that showed positive results for the presence of coliforms were submitted to three dilutions (10^{-1} , 10^{-2} and 10^{-3}) and subdivided into three groups comprising three tubes with their own culture medium.

The presumptive test for coliforms was performed using Lauril Sulfate Triptose (LST) broth enriched with 50 mg L^{-1} of 4-methylumbelliferyl- β -D-glucuronide (LST-MUG). The analyses were performed by pipetting 1.0 mL aliquots of different dilutions into a series of three tubes containing 9.0 mL of LST-MUG and provided with an inverted Durham tube, homogenized and incubated at 35°C for 48 h. Gas production observed in the Durham tubes indicated the presence of coliforms.

Following the 24 h incubation at 37°C using the serial tube methodology, all the LST-MUG tubes that exhibited fluorescence were considered positive for *E. coli* when exposed to ultraviolet light (6W) with a long wavelength (366 nm) in a dark room.

The *E. coli* solution was prepared using the strain cultured in TSB broth. Then, 200 μL of such solution were dispensed into a tube containing 3.0 mL of a 0.85% NaCl solution (mass percentage). Afterwards, the turbidity corresponding to 0.5 on the McFarland scale (10^9 bacteria mL^{-1}) was determined. The solution obtained was subjected to antimicrobial susceptibility tests by the plate diffusion method (Müller Hinton Agar) and the polymer matrix containing the AgNPs were transferred into the plates and incubated for 24 h at 25°C . The antimicrobial activity of the pellets impregnated with silver nanoparticles was assessed by the most probable number (MPN), according to the ASTM International (2001).

The tests were carried out using 2.0 g of PA/AgNPs pellets containing 0.05, 0.10 and 0.50% (m/m) of silica powder functionalized with the metal nanostructures. Three triplicate samples comprising 2.0 g of pellets without silver nanoparticles were used as control.

Subsequently, 1.0 g of inoculum was solubilized in 50 mL of deionized water at a concentration of $2.0\text{-}3.0 \times 10^5$ CFU mL^{-1} . The flasks were closed and incubated in a shaking oven with temperature controlled at 25°C for 24 h. Several dilutions were prepared from 1.0 mL from each vial. All tests were performed in triplicate. The microbial reduction percentage was calculated by Equation 1.

$$\text{Reduction \%} \left(\frac{UFC}{ml} \right) = \frac{B-A}{B} \times 100 \quad (1)$$

where: A is the microbial count in the sample containing (AgNPs) (CFU/mL) and B is the microbial count in the sample with no antibacterial agent (control).

The samples were stirred at $40 \pm 2 \text{ min}^{-1}$ for 20 h on a magnetic stirrer. Afterwards, the samples were vacuum-filtered and the liquid fraction was subjected to inductively coupled plasma atomic mass spectroscopy (ICP-MS) to quantify the silver leached from the PA/AgNPs pellets.

2.5. Statistical analysis and *E. coli* reduction kinetics

The data were treated by analysis of variance (ANOVA) and Tukey's test at 5% of significance using Statistica for Windows (Version 7.0, Statsoft). The results allowed determining the reduction kinetics of *E. coli* under two different conditions: agitation and no agitation of the solution added with AgNPs. The reaction order was determined by the Pearson correlation coefficient, R^2 , which measures the degree of linear correlation between two quantitative variables, yielding values between 0 and 1.

3. RESULTS AND DISCUSSION

Figure 2 shows a transmission electron microscopy (TEM) image of the silver nanoparticles. The synthesized nanostructures exhibited an approximate spherical shape, with an average size between 20 and 30 nm.

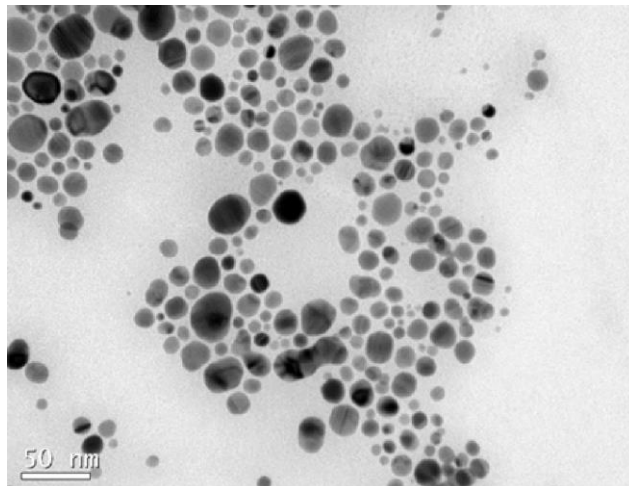


Figure 2. MET image ($\times 450,000$ times).

The absorbance spectrum shown in Figure 3 shows a peak absorbance close to 400 nm. Similar results were published in Nogueira et al. (2014; 2016), who reported that silver nanoparticles with predominantly spherical shape presented a surface plasmon resonance that absorbs the radiation at wavelength around 400 nm in the UV-visible region.

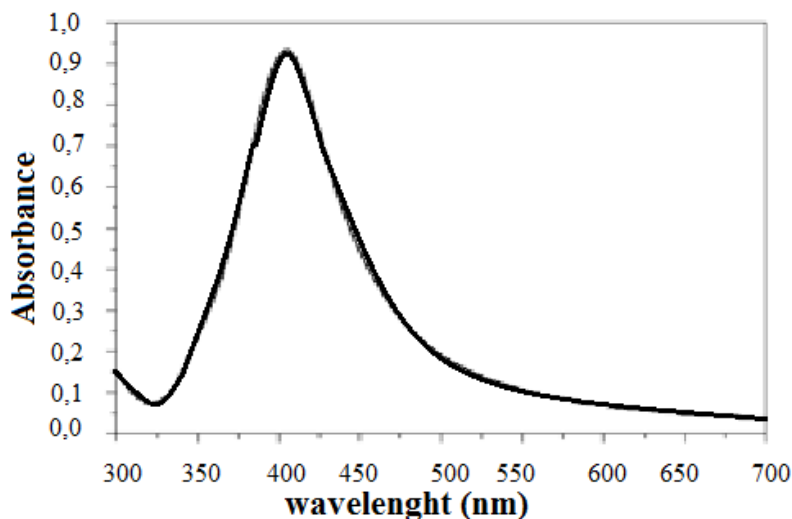


Figure 3. Absorption spectrum of synthesized silver nanoparticles.

The silica microparticles with adsorbed silver nanoparticles were also analysed by transmission electron microscopy. The images presented in Figure 4 show that the metallic nanostructures are well dispersed on the silica's surface. Figure 4a, a conventional image without contrast, shows the nanoparticles as dark spots. In Figure 4b, to which an optical contrast feature was applied, the bright dots indicate the presence of a metallic material adsorbed on the surface of the silica microparticles. This metallic material corresponds to the silver nanoparticles, which reflect part of the incident electron beam.

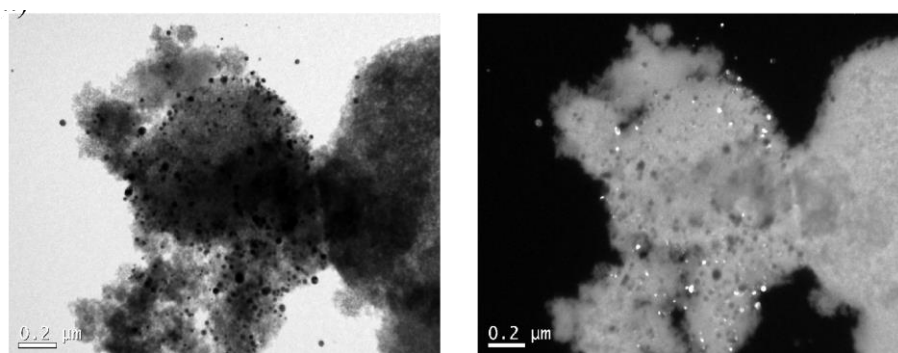


Figure 4. MET image of the silver nanoparticles adsorbed on the silica surface: a) without contrast; b) with contrast.

The following average values were obtained from the silver-leaching tests as a function of the amount of functionalized silica incorporated in the polyamide: 0.052 mg L⁻¹ (0.50%), 0.020 mg L⁻¹ (0.10%) and 0.008 mg L⁻¹ (0.05%). The polyamide sample that complied with the maximum limit of leached silver as established in the Conama resolution 357/2005 (CONAMA, 2005) (0.010 mg L⁻¹) was used in the microbiological tests. The tests were performed with pellets containing 0.05% by weight of silica powder functionalized with silver nanoparticles.

The antibacterial activity was determined in terms of mean faecal contamination (CFU m L⁻¹). The tests were carried out in triplicate and the Tukey test was used to analyse the bactericidal effect of the pellets containing silver nanoparticles (N) on the representative Gram-negative bacteria (*E. coli*) after exposure times of 1 h, 2 h and 3 h. AgNP-free samples were used as control. The data summarized in Table 1 indicate that the averages followed by the same letter in the columns do not differ by the Tukey test (Tt) at 5% significance level.

Table 1. Faecal coliform (*E. coli*) contamination (average ± standard deviation) of different samples.

Sample PA/AgNps	CFU mL ⁻¹	Tt	Control	Tt	CFU mL ⁻¹
NA251	1.67 ± 2.08	d	BA251	ef	6.10 ± 1.05
NA252	1.33 ± 1.53	d	BA252	ef	19.07 ± 7.22
NA253	1.00 ± 1.73	ed	BA253	c	47.17 ± 11.77
NSA251	28.50 ± 1.31	ef	BSA251	b	61.60 ± 1.49
NSA252	23.83 ± 1.10	f	BSA252	a	90.27 ± 4.91
NSA253	16.07 ± 5.33	f	BSA253	b	70.00 ± 2.00

Legend: N = silver nanoparticles; B = control (no nanoparticles); A= stirring; SA= no stirring; Tt= Tukey test (5% significance level).

Table 1 shows the interaction between residence time and stirring. A significant microbial reduction to final concentrations of 1.33 CFU mL⁻¹ (NA252) and 1.00 CFU mL⁻¹ (NA253) were reached in the presence of silver nanoparticles for residence times of 2 h and 3 h, respectively. In Table 1, averages followed by the same letter in the same columns do not differ by the Tukey test at a 5% significance level. The control (BSA252) reached an average *E. coli* count of 90.27 CFU mL⁻¹ in 2 h. The reduction in the presence of silver nanoparticles (NA252) for the same residence time was 93.05% (p < 0.05). The antimicrobial activity is ascribed to the action of silver ions on the respiratory chain of bacteria, by decoupling the electron transfer in oxidative phosphorylation, thereby inhibiting the enzymes of the respiratory chain (Feng et al., 2000). Figure 5 shows the reduction kinetics of *E. coli* attributed to the antibacterial activity of silver nanoparticles.

Figure 5 shows the mean percentage of microbial reduction ascribed to the antibacterial activity of silver nanoparticles incorporated in polyamide-66. The lowest antibacterial reduction

occurred for sample NSA251 (53.73%), no stirring and 1 h contact time. The most significant reduction was observed for sample NA253 (97.89%), corresponding to stirring and 3 h contact time.

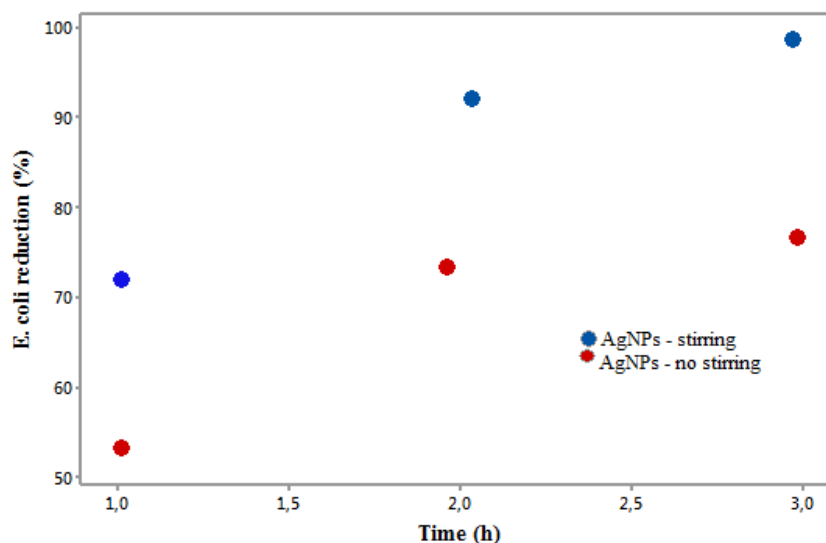


Figure 5. Reduction kinetics of *E. coli*.

The microbiological analysis revealed that both conditions (stirring and no stirring), result in a relevant bactericidal effect, as stated by Tan et al. (2015). Some authors confirm that AgNPs establish chemical bonds with sulphur and phospholipids present in the DNA, inhibiting various cellular processes in gram-negative bacteria (Franci et al., 2015; Li et al., 2011; Morones et al., 2005). The changes are associated with adverse effects resulting from the antibacterial activity of AgNPs in the cell membrane due to increased production of reactive oxygen species (ROS) (Franci et al., 2015).

The cellular stress mediated by reactive oxygen species has a detrimental and irreversible effect on the intracellular structure of bacteria (Morones et al., 2005; Choi and Hu, 2008). Xu et al. (2012) reported that some reactive oxygen species (ROS), including superoxide ($\bullet\text{O}_2^-$), hydrogen peroxide (H_2O_2) and hydroxyl radical ($\bullet\text{OH}$), are generated during aerobic metabolism.

The chemical interaction between AgNPs and the cell membrane of bacteria can be related to the presence of sulphur in proteins, forming preferential sites with AgNPs (Zhang et al., 2013). Therefore, exposure to AgNPs promotes an increase in the rate of lipid peroxidation and oxidation of the protein due to lesser thiol groupings ($-\text{SH}$) bounded to protein (Struzyński et al., 2014). The reduction of thiol levels and glutathione activity may induce AgNP-exposed organisms to ineffective antioxidant mechanisms against cellular stress mediated by reactive oxygen species (Becaro et al., 2015).

When stirring was used, the bacterial activity was reduced exponentially as R^2 approached 1.0. It was possible to obtain a trend line with a very satisfactory correlation coefficient of 0.9973, according to Equation 2.

$$y = 0.1631e^{0.5574x} \quad (2)$$

where: t is the residence time (h).

Equation 2 represents the exponential microbial reduction as a function of the initial concentration of the indicator bacterium, time and bacterial reduction rate. Equation 2 allows prediction of the bacterial reduction without the use of stirring in any residence time.

The Pearson coefficient was 0.9349 for the tests without stirring. Equation 3 represents the exponential curve of the sample behaviour in these conditions.

$$y = 0.1358e^{0.5295x} \quad (3)$$

4. CONCLUSIONS

Functional nanoparticles supported in a polymeric matrix were proved an efficient bacterial inhibitor for water disinfection. The results concerning the leaching tests indicate that the concentration of 0.05% AgNPs in the polymer matrix met the maximum value allowed by the current legislation (Conama 357/2005), which is 0.010 mg.L⁻¹. The most significant reduction (97.89%) was observed for the sample with AgNPs, stirring and 3 h contact time. The antibacterial reduction related to stirring can be explained by the high surface area/volume ratio of the silver nanoparticles, which in theory yield a greater diffusive contact between the AgNPs and the bacteria, allowing a fast release of Ag⁺ and consequent reduction of antibacterial activity. A longer diffusive contact time between silver nanoparticles and the studied bacteria results in structural alterations and deformations in the membrane walls and nucleic acids of the bacterial cells.

5. REFERENCES

- ALIZADEH, H.; SALOUTI, M.; SHAPOURI, R. Bactericidal effect of silver nanoparticles on intramacrophage brucella abortus 544. **Jundishapur Journal of Microbiology**, v. 7, n. 3, 2014. <https://dx.doi.org/10.5812%2Fjjm.9039>
- AMERICAN PUBLIC HEALTH ASSOCIATION. **Standard methods for the examination of water and wastewater**. 22. ed. Washington, D.C., 2012. p. 9-70.
- ARAÚJO, K. S.; ANTONELLI, R.; GAYDECZKA, B.; GRANATO, A. C.; MALPASS, G. R. P. Processos oxidativos avançados: uma revisão de fundamentos e aplicações no tratamento de águas residuais urbanas e efluentes industriais. **Revista Ambiente & Água**, v. 11, n. 2, p. 387-401, 2016. <http://dx.doi.org/10.4136/ambi-agua.1862>
- ASTM INTERNATIONAL. **E 2149 Standard test method for determining the antimicrobial activity of immobilized antimicrobial agents under dynamic contact conditions**. West Conshohocken, 2001.
- BECARO, A. A.; PUTI, F. C.; CORREA, D. S.; PARIS, E. C.; MARCONCINI, J. M.; FERREIRA, M. D. Polyethylene films containing silver nanoparticles for applications in food packaging: characterization of physico-chemical and anti-microbial properties. **Journal of nanoscience and nanotechnology**, v. 15, n. 3, p. 2148-2156, 2015. <https://doi.org/10.1166/jnn.2015.9721>
- CHOI, O.; HU, Z. Size dependent and reactive oxygen species related nanosilver toxicity to nitrifying bacteria. **Environmental science & technology**, v. 42, n. 12, p. 4583-4588, 2008. <http://dx.doi.org/10.1021/es703238h>
- CONSELHO NACIONAL DO MEIO AMBIENTE (Brasil). Resolução n° 357/05. Estabelece a classificação das águas doces, salobras e salinas do Território Nacional. **Diário Oficial [da] União**, Brasília, n. 53, de 18 mar. 2005, p. 58-63.
- DURÁN, N.; DURÁN, M.; DE JESUS, M. B.; SEABRA, A. B.; FÁVARO, W. J.; NAKAZATO, G. Silver nanoparticles: a new view on mechanistic aspects on antimicrobial activity. **Nanomedicine: Nanotechnology, Biology and Medicine**, v. 12, n. 3, p. 789-799, 2016. <https://doi.org/10.1016/j.nano.2015.11.016>

- FENG, Q. L.; WU, J.; CHEN, G. Q.; CUI, F. Z.; KIM, T. N.; KIM, J. O. A mechanistic study of the antibacterial effect of silver ions on *Escherichia coli* and *Staphylococcus aureus*. **Journal of biomedical materials research**, v. 52, n. 4, p. 662-668, 2000. [https://doi.org/10.1002/1097-4636\(20001215\)52:4<662::AID-JBM10>3.0.CO;2-3](https://doi.org/10.1002/1097-4636(20001215)52:4<662::AID-JBM10>3.0.CO;2-3)
- FRANCI, G.; FALANGA, A.; GALDIERO, S.; PALOMBA, L.; RAI, M.; MORELLI, G. et al. Silver nanoparticles as potential antibacterial agents. **Molecules**, v. 20, n. 5, p. 8856-8874, 2015. <http://dx.doi.org/10.3390/molecules20058856>
- KIM, H.; KIM, Y., KIM, Y.; LEE, S. Removal of ZnO Nanoparticles in Aqueous Phase and Its Ecotoxicity Reduction. **Clean Technology**, v. 22, n. 2, p. 89-95, 2016. <https://doi.org/10.7464/ksct.2016.22.2.089>
- LI, M.; ZHU, L.; LIN, D. Toxicity of ZnO nanoparticles to *Escherichia coli*: mechanism and the influence of medium components. **Environmental Science & Technology**, v. 45, p. 1977-1983, 2011. <http://dx.doi.org/10.1021/es102624t>
- MORONES, J. R.; ELECHIGUERRA, J. L.; CAMACHO, A.; HOLT, K.; KOURI, J. B.; RAMÍREZ, J. T. et al. The bactericidal effect of silver nanoparticles. *Nanotechnology*, v. 16, p. 2346-2353, 2005. <https://doi.org/10.1088/0957-4484/16/10/059>
- MOHANTY, S.; MISHRA, S.; JENA, P.; JACOB, B.; SARKAR, B.; SONAWANE, A. An investigation on the antibacterial, cytotoxic, and antibiofilm efficacy of starch-stabilized silver nanoparticles. **Nanomedicine: Nanotechnology, Biology and Medicine**, v. 8, p. 916-924, 2012. <https://doi.org/10.1016/j.nano.2011.11.007>
- NASCIMENTO, S. F. V.; ARAÚJO, F. F. M. Ocorrência de bactérias patogênicas oportunistas em um reservatório do semiárido do Rio Grande do Norte, Brasil. **Revista de Ciências Ambientais-RCA**, v. 7, p. 91-104, 2013. <http://dx.doi.org/10.18316/1080>
- NOGUEIRA, A. L.; MACHADO, R. A.; de SOUZA, A. Z.; MARTINELLO, F.; FRANCO, C. V.; DUTRA, G. B. Synthesis and characterization of silver nanoparticles produced with a bifunctional stabilizing agent. **Industrial & Engineering Chemistry Research**, v. 53, p. 3426-3434, 2014. <http://dx.doi.org/10.1021/ie4030903>
- NOGUEIRA, A. L.; MACHADO, R. A.; de SOUZA, A. Z.; FRANCO, C. V.; DUTRA, G. B. Influence of process parameters and scalability of the semi-batch production of functionalized silver nanoparticles. **The Canadian Journal of Chemical Engineering**, v. 94, n. 8, p. 1472-1485, 2016. <https://doi.org/10.1002/cjce.22530>
- POLTE, J.; TUAEV, X.; WUITHSCHICK, M.; FISCHER, A.; TGUENEMANN, A. F.; RADEMANN, K. et al. Formation mechanism of colloidal silver nanoparticles: analogies and differences to the growth of gold nanoparticles. **Acs Nano**, v. 6, n. 7, p. 5791-5802, 2012. <http://dx.doi.org/10.1021/nn301724z>
- STRUŻYŃSKI, W.; DĄBROWSKA-BOUTA, B.; GRYGOROWICZ, T.; ZIEMIŃSKA, E.; STRUŻYŃSKA, L. Markers of oxidative stress in hepatopancreas of crayfish (*Orconectes limosus*, raf) experimentally exposed to nanosilver. **Environmental toxicology**, v. 29, n. 11, p. 1283-1291, 2014. <http://dx.doi.org/10.1002/tox.21859>
- TAN, Z. Q.; LIU, J. F.; GUO, X. R.; YIN, Y. G.; BYEON, S. K.; MOON, M. H. et al. Toward full spectrum speciation of silver nanoparticles and ionic silver by on-line coupling of hollow fiber flow field-flow fractionation and minicolumn concentration with multiple detectors. **Analytical Chemistry**, v. 87, n. 16, p. 8441-8447, 2015. <http://dx.doi.org/10.1021/acs.analchem.5b01827>

- VÖRÖSMARTY, C. J.; GREEN, P.; SALISBURY, J.; LAMMERS, R. B. Global water resources: vulnerability from climate change and population growth. **Science**, v. 289, p. 284-288, 2000. <http://dx.doi.org/10.1126/science.289.5477.284>
- XU, H.; QU, F.; XU, H.; LAI, W.; WANG, Y. A.; AGUILAR, Z. P. et al. Role of reactive oxygen species in the antibacterial mechanism of silver nanoparticles on Escherichia coli O157: H7. **Biometals**, v. 25, n. 1, p. 45-53, 2012. <https://doi.org/10.1007/s10534-011-9482-x>
- ZHANG, H.; OYANEDEL-CRAVER, V. Comparison of the bacterial removal performance of silver nanoparticles and a polymer based quaternary amine functionalized silsesquioxane coated point-of-use ceramic water filters. **Journal of Hazardous Material**, v. 260, p. 272-277, 2013. <http://dx.doi.org/10.1016/j.jhazmat.2013.05.025>
- ZHANG, W.; LI, Y.; NIU, J.; CHEN, Y. Photogeneration of reactive oxygen species on uncoated silver, gold, nickel, and silicon nanoparticles and their antibacterial effects. **Langmuir**, v. 29, n.15, p. 4647-4651, 2013. <http://dx.doi.org/10.1021/la400500t>